Long Range 1,4 and 1,6-Interstrand Cross-Links Formed by a Trinuclear Platinum Complex. Minor Groove Preassociation Affects Kinetics and Mechanism of Cross-Link Formation as Well a...

ARTICLE *in* JOURNAL OF THE AMERICAN CHEMICAL SOCIETY · MARCH 2004

Impact Factor: 12.11 · DOI: 10.1021/ja036105u · Source: PubMed

6 AUTHORS, INCLUDING:

Donald S. Thomas
University of New South Wales
30 PUBLICATIONS **417** CITATIONS

SEE PROFILE

J|A|C|S
ARTICLES
Published on Web 01/29/2004

Long Range 1,4 and 1,6-Interstrand Cross-Links Formed by a Trinuclear Platinum Complex. Minor Groove Preassociation Affects Kinetics and Mechanism of Cross-Link Formation as Well as Adduct Structure

Alexander Hegmans,[‡] Susan J. Berners-Price,*[,†] Murray S. Davies,[†,§] Donald S. Thomas,[†] Anthony S. Humphreys,[†] and Nicholas Farrell*[,‡]

Contribution from the Department of Chemistry, University of Western Australia, Crawley, WA, 6009, Australia, and the Department of Chemistry, Virginia Commonwealth University, Richmond, Virginia 23284-2006

Received May 13, 2003; E-mail: sbp@chem.uwa.edu.au; nfarrell@mail1.vcu.edu

Abstract: Reported here is a comparison of the kinetics of the stepwise formation of 1,4- and 1,6-GG interstrand cross-links by the trinuclear platinum anticancer compound ^{15}N-[{*trans*-PtCl(NH$_3$)$_2$}$_2${μ-*trans*-Pt(NH$_3$)$_2$(H$_2$N(CH$_2$)$_6$NH$_2$)$_2$}]$^{4+}$, (1,0,1/t,t,t (**1**) or BBR3464). The reactions of ^{15}N-**1** with the self-complementary 12-mer duplexes 5′-{d(ATAT**G**TACATAT)$_2$} (**I**) and 5′-{d(TAT**G**TATACATA)$_2$} (**II**) have been studied at 298 K, pH 5.3 by [^{1}H,^{15}N] HSQC 2D NMR spectroscopy. The kinetic profiles for the two reactions are similar. For both sequences initial electrostatic interactions with the DNA are observed for **1** and the monoaqua monochloro species (**2**) and changes in the chemical shifts of certain DNA ^{1}H resonances are consistent with binding of the central charged {PtN$_4$} linker unit in the minor groove. The pseudo first-order rate constants for the aquation of **1** to **2** in the presence of duplex **I** ($3.94 \pm 0.03 \times 10^{-5}$ s^{-1}), or **II** ($4.17 \pm 0.03 \times 10^{-5}$ s^{-1}) are ca. 40% of the value obtained for aquation of **1** under similar conditions in the absence of DNA. Monofunctional binding to the guanine N7 of the duplex occurs with rate constants of 0.25 ± 0.02 M^{-1} s^{-1} (**I**) and 0.34 ± 0.02 M^{-1} s^{-1} (**II**), respectively. Closure to form the 1,4- or 1,6-interstrand cross-links (**5**) was treated as direct from **3** with similar rate constants of $4.21 \pm 0.06 \times 10^{-5}$ s^{-1} (**I**) and $4.32 \pm 0.04 \times 10^{-5}$ s^{-1} (**II**), respectively. Whereas there is only one predominant conformer of the 1,6 cross-link, evidence from both the ^{1}H and [^{1}H,^{15}N] NMR spectra show formation of two distinct conformers of the 1,4 cross-link, which are not interconvertible. Closure to give the major conformer occurs 2.5-fold faster than for the minor conformer. The differences are attributed to the initial preassociation of the central linker of **1** in the minor groove and subsequently during formation of both the monofunctional and bifunctional adducts. For duplex **I**, molecular models indicate two distinct pathways for the terminal {PtN$_3$Cl} groups to approach and bind the guanine N7 in the major groove with the central linker anchored in the minor groove. To achieve platination of the guanine residues in duplex **II** the central linker remains in the minor groove but **1** must diffuse off the DNA for covalent binding to occur. Clear evidence for movement of the linker group is seen at the monofunctional binding step from changes of chemical shifts of certain CH$_2$ linker protons as well as the Pt−NH$_3$ and Pt−NH$_2$ groups. Consideration of the ^{1}H and ^{15}N shifts of peaks in the Pt−NH$_2$ region show that for both the 1,4 and 1,6 interstrand cross-links there is a gradual and irreversible transformation from an initially formed conformer(s) to product conformer(s) in which the amine protons of the two bound {PtN$_3$} groups exist in a number of different environments. The behavior is similar to that observed for the 1,4-interstrand cross-link of the dinuclear 1,1/t,t compound. The potential significance of preassociation in determining kinetics of formation and structure of the adducts is discussed. The conformational flexibility of the cross-links is discussed in relation to their biological processing, especially protein recognition and repair, which are critical determinants of the cytotoxicity of these unique DNA-binding agents.

Introduction

The trinuclear complex [(*trans*-PtCl(NH$_3$)$_2$)$_2${μ-*trans*-Pt(NH$_3$)$_2$(H$_2$N(CH$_2$)$_6$NH$_2$)$_2$}]$^{4+}$, (1,0,1/t,t,t (**1**) or BBR3464) has undergone Phase II clinical trials for treatment of a variety of cancers.[1] The agent is the lead example of a genuinely new structural class of anticancer drugs, based on the multinuclear

[†] University of Western Australia.
[‡] Department of Chemistry, VCU.
[§] Present address: School of Pharmacy and Molecular Sciences, James Cook University, Townsville QLD, 4811, Australia.

(1) Calvert, A. H.; Thomas, H.; Colombo, N.; Gore, M.; Earl, H.; Sena, L.; Camboni, G.; Liati, P.; Sessa, C. *Eur. J. Cancer* **2001**, *37* (Supp6), Poster 965. Scagliotti, G.; Crinò, L.; De Marinis, F.; Tonato, M.; Selvaggi, G.; Massoni, F.; Maestri, A.; Gatti, B.; Camboni, G. *Eur. J. Cancer* **2001**, *37* (Supp6), Poster 182.

10.1021/ja036105u CCC: $27.50

platinum motif, where two or more platinum coordination units are linked by flexible diamine(polyamine) linkers.[2] Multinuclear platinum complexes are structurally very diverse[3] and the subclass of most interest is represented by the generic structure:

Scheme 1. General Structure Diagram for Di- and Trinuclear Complexes

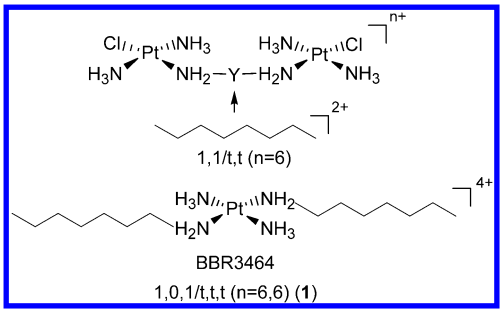

The presence of charge and hydrogen-bonding capacity within the central linker (either in the form of a tetraamineplatinum moiety as in **1** or a charged polyamine linker such as spermidine or spermine) produces compounds significantly more potent than the "simple" dinuclear species represented by the 1,1/t,t compound above.[2] In all cases, bifunctional DNA binding is achieved by two independent monofunctional platinum coordination spheres, eliminating many of the steric requirements when two nucleobases are bound to one Pt, as for cisplatin and congeners. Long-range intra- and interstrand cross-links, where the sites of platination may be separated by up to four base pairs, are the predominant lesions formed by multinuclear platinum complexes. The presence of charge in the linker enhances the kinetics of DNA binding in globally platinated DNA, as well as affecting the relative ratios and the nature of intra and inter-strand cross-links.[4,5]

A further distinction is that the greater distance between the platinating moieties in 1,0,1/t,t,t allows for even longer-range cross-links—molecular modeling and analysis of stop-sites on DNA and RNA polymerase indicate that for the trinuclear compound 1,6-cross-links are also easily achievable.[4,6] Kinetic studies using gel electrophoresis show that the rate of formation of the 1,6 cross-link is slower than that of the 1,4[6] and that such a 1,6-cross-link would be unlikely to be formed by the 1,1/t,t compound because of the distance between the two guanines.[4] 1,6 cross-links across the major groove are very rare,[7] although formal analogy may be drawn to the 1,6-interstrand cross-links formed by the antibiotic bizelesin—in this case the cross-link is located in the minor groove following alkylation of Adenine N3 positions.[8]

DNA binding is likely to contribute to the antitumor activity of platinum agents.[9] Comparison of the details of DNA binding between the dinuclear and trinuclear compound may help delineate the features responsible for the remarkable potency of the latter, and especially the contribution of the hydrogen-bonding and electrostatic interactions of the central noncovalent platinum moiety. As part of the broad examination of the properties and biological consequences of polynuclear Pt-DNA adducts, we have used [^{1}H,^{15}N] HSQC NMR spectroscopy to probe the aquation and DNA binding kinetics of prototype dinuclear[10−13] and trinuclear[14] complexes. In this way, it is possible to observe all platinated species at low (μM) concentrations because only ^{1}H and ^{15}N resonances derived from platinum am(m)ine species are seen. These methods have provided new insight into the kinetics and mechanism of DNA binding by cisplatin and other mononuclear analogues.[15] [^{1}H,^{15}N] HSQC NMR is proving to be especially useful for following the reactions of multinuclear systems because ^{15}N-labeling of both $^{15}NH_2$ and $^{15}NH_3$ groups is possible. The spectra are considerably more complicated than those observed for cisplatin, but the NH_2 and NH_3 regions of the [^{1}H,^{15}N] 2D NMR spectra are well separated, allowing the reaction to be followed independently in each region. An additional feature of the technique is that the ^{1}H and ^{15}N shifts are sensitive to H-bonding interactions with DNA and thus the role of the central linker of 1,0,1/t,t,t (**1**) can be probed at every stage of the process, as well as the terminal units responsible for platination.

Study of the aquation of ^{15}N labeled 1,0,1/t,t,t (**1**) and 1,1/t,t has shown that the equilibria favor strongly the dichloro form.[10,14] For the trinuclear compound the aquation rate constant is comparable to 1,1/t,t, but the chloride anation rate constant is lower so that there is a significantly greater percentage of aquated species (ca. 30%) present at equilibrium. The pK_a of the aqua ligands in both compounds is identical (pK_a 5.62) and much lower than for *cis*-$[PtCl(H_2O)(NH_3)_2]^+$ (pK_a 6.41).[16] For the dinuclear 1,1/t,t complex we were able to follow the stepwise formation of a long-range DNA 1,4-interstrand cross-link on the duplex 5′-{d(ATAT**G**TACATAT)$_2$} (**I**) and derive kinetic parameters for each step in the pathway.[11] Changes in the ^{1}H and ^{15}N shifts of the bifunctional interstrand cross-link showed

(2) Farrell, N.; Qu, Y.; Bierbach, U.; Valsecchi, M.; Menta, E. In *Cisplatin: Chemistry and Biochemistry of a Leading Anticancer Drug*; Lippert, B., Ed.; VCHA, Wiley-VCH: Zurich, 1999; pp 479−496. Farrell, N. In *Platinum Based Drugs in Cancer Therapy*; Kelland, L. R., Farrell, N., Eds.; Humana Press: Totawa NJ, 2000; pp 321−338. Manzotti, C.; Pratesi, G.; Menta, E.; Di Domenico, R.; Cavaletti, E.; Fiebig, H. H.; Kelland, L. R.; Farrell, N.; Polizzi, D.; Supino, R.; Pezzoni, G.; Zunino, F. *Clin. Cancer Res.* **2000**, *6*, 2626−2634.
(3) Qu, Y.; Rauter, H.; Soares Fontes, A. P.; Bandarage, R.; Kelland, L. R.; Farrell, N. *J. Med. Chem.* **2000**, *43*, 3189−3192.
(4) Brabec, V.; Kasparková, J.; Vrána, O.; Nováková, O.; Cox, J. W.; Qu, Y.; Farrell, N. *Biochemistry* **1999**, *38*, 6781−6790.
(5) McGregor, T. D.; Kasparkova, J.; Neplechova, K.; Novakova, O.; Penazova, H.; Vrana, O.; Brabec, V.; Farrell, N. *J. Biol. Inorg. Chem.* **2002**, *7*, 397−404.
(6) Kasparková, J.; Zehnulova, J.; Farrell, N.; Brabec, V. *J. Biol. Chem.* **2002**, *277*, 48 076−48 086.
(7) Rajski, S. R.; Williams, R. M. *Chem. Rev.* **1998**, *98*, 2723−2795.
(8) Woynarowski, J. M.; Chapman, W. G.; Napier, C.; Herzig, M. C. S. *Biochim. Biophys. Acta* **1999**, *1444*, 201−217. Lee, M.; Roldan, M. C.; Haskell, M. K.; McAdam, S. R.; Hartley, J. A. *J. Med. Chem.* **1994**, *37*, 1208−1213. Woynarowski, J. M.; McHugh, M.; Gawron, L. S.; Beerman, T. A. *Biochemistry* **1995**, *34*, 13042−13050. Sun, D.; Hurley, L. H. *J. Am. Chem. Soc.* **1993**, *115*, 5925−5933.
(9) Kelland, L. R., Farrell, N., Eds.; *Platinum-Based Drugs in Cancer Therapy*; Humana Press: 2000. Lippert, B., Ed.; *Cisplatin: Chemistry and Biochemistry of a Leading Anticancer Drug*; VCHA, Wiley-VCH: Zurich, 1999. Cohen, S. M.; Lippard, S. J. *Prog. Nucl. Acids Res Mol. Biol.* **2001**, *67*, 93−130. Brabec, V. *Prog. Nucl. Acids. Res. Mol. Biol.* **2002**, *71*, 1−68.
(10) Davies, M. S.; Cox, J. W.; Berners-Price, S. J.; Barklage, W.; Qu, Y.; Farrell, N. *Inorg. Chem.* **2000**, *39*, 1710−1715.
(11) Cox, J. W.; Berners-Price, S. J.; Davies, M. S.; Farrell, N.; Qu, Y. *J. Am. Chem. Soc.* **2001**, *123*, 1316−1326.
(12) Berners-Price, S. J.; Davies, M. S.; Cox, J. W.; Thomas, D. S.; Farrell, N. *Chem.−Eur. J.* **2003**, *9*, 713−725.
(13) Davies, M. S.; Berners-Price, S. J.; Cox, J. W.; Farrell, N. *Chem. Commun.* **2003**, 122−123.
(14) Davies, M. S.; Thomas, D. S.; Hegmans, A.; Berners-Price, S. J.; Farrell, N. *Inorg. Chem.* **2002**, *41*, 1101−1109.
(15) Davies, M. S.; Berners-Price, S. J.; Hambley, T. W. *J. Am. Chem. Soc.* **1998**, *120*, 11380−11390. Berners-Price, S. J.; Barnham, K. J.; Frey, U.; Sadler, P. J. *Chem.−Eur. J.* **1996**, *2*, 1283−1291. Murdoch, P. del. S.; Guo, Z.; Parkinson, J. A.; Sadler, P. J. *J. Biol. Inorg. Chem.* **1999**, *4*, 32−38. Reeder, F.; Guo, Z.; Murdoch, P. del S.; Corazza, A.; Hambley, T. W.; Berners-Price, S. J.; Chottard, J. C.; Sadler, P. J. *Eur. J. Biochem* **1997**, *249*, 370−382.
(16) Berners-Price, S. J.; Frenkiel, T. A.; Frey, U.; Ranford, J. D.; Sadler, P. J. *J. Chem. Soc., Chem. Commun.* **1992**, 789−791.

evidence for irreversible transformation of an initially formed conformer(s) to product conformer(s).

In this paper, we compare the kinetics of binding of the trinuclear complex **1** to the same duplex under identical conditions and compare the nature of the 1,4-interstrand cross-links formed. We also examine the kinetics and formation of a "longer" 1,6-cross-link within the sequence 5′-{d(TAT**G**TATA-CATA)$_2$} (**II**) to delineate the similarities and/or differences with the 1,4-case. The presence of an extra set of (AT) base pairs within the sequence influences the preassociation of the drug with the DNA. The nature of the preassociation and its effect on kinetics of cross-link formation as well as on adduct profile and structure are discussed.

Experimental Section

Chemicals. The sodium salts of the HPLC purified oligonucleotides 5′-(ATAT**G**TACATAT)-3′ (**I**) and 5′-(TAT**G**TATACATA)-3′ (**II**) were purchased from OSWEL. The nitrate salt of the fully ^{15}N labeled [{*trans*-PtCl(^{15}NH$_3$)$_2$}{μ-*trans*-Pt(^{15}NH$_3$)$_2$(^{15}NH$_2$-(CH$_2$)$_6$-^{15}NH$_2$)$_2$}]$^{4+}$ (1,0,1/t,t,t; ^{15}N-**1**) was prepared according to the reported synthesis of the unlabeled compound by using ^{15}N labeled *trans*-PtCl$_2$(^{15}NH$_3$)$_2$ and ^{15}NH$_2$-(CH$_2$)$_6$-^{15}NHBOC, respectively.[14]

Sample Preparation. Stock solutions of duplexes **I** and **II** were prepared in 300−500 μL of 5% D$_2$O in H$_2$O. The duplex concentrations were estimated spectrophotometrically to be 15.6 mM (**I**) and 13.2 mM (**II**), respectively based on the absorption coefficient of $\epsilon_{260} = 186.35 \times 10^3$ M^{-1} cm^{-1} for these sequences derived using the method of Kallansrud and Ward.[17]

Reaction of Duplex I with ^{15}N-1. 76 μL of the stock solution of 5′-d(ATAT**G**TACATAT)-3′ (15.6 mM duplex), 30 μL sodium phosphate buffer (200 mM, pH 5.3) and 2 μL of TSP solution (sodium-3-trimethylsilyl-D$_4$-propionate, 13.3 mM) were combined in 272 μL 5% D$_2$O/95% H$_2$O. The duplex was melted in a water bath (330−340 K) and then slowly allowed to cool to room temperature. A 20-μL aliquot of a freshly prepared solution of fully labeled ^{15}N-**1** (1.50 mg, 1.20 μmol) in 37.5 μL 5% D$_2$O/95% H$_2$O was added to the duplex to reach a volume of 400 μL, with final concentrations of duplex (2.96 mM), phosphate buffer (15 mM) and ^{15}N-**1** (1.60 mM). The reaction was carried out at 298 K and was followed by ^{1}H and [^{1}H,^{15}N] NMR over a total time of 45 h. The final pH of the solution was 5.9.

A control sample of the same complex concentration was prepared by combining 30 μL sodium phosphate buffer (200 mM, pH 5.3), 2 μL of TSP solution and 348 μL 5% D$_2$O/95% H$_2$O with fully ^{15}N labeled **1** (0.80 mg, 0.64 μmol) dissolved in 20 μL H$_2$O.

Reaction of Duplex II with ^{15}N-1. 84 μL of the stock solution of 5′-d(TAT**G**TATACATA)-3′ (13.2 mM duplex), 33 μL sodium phosphate buffer (200 mM, pH 5.3) and 2 μL of TSP solution were combined in 281 μL 5% D$_2$O/95% H$_2$O. 20 μL of the solution were removed for pH and UV absorption measurements. A melting profile of the duplex was obtained by taking ^{1}H NMR spectra in the range between 298 and 318 K in increments of 5 K. The duplex was then allowed to come to room temperature and a 40 μL aliquot of a freshly prepared solution of ^{15}N-**1** (1.14 mg, 0.91 μmol) in 46 μL 5% D$_2$O was added to the duplex to reach a total volume of 420 μL, with final concentrations of duplex (2.62 mM), phosphate buffer (15 mM) and ^{15}N-**1** (1.9 mM). The reaction was followed by ^{1}H and [^{1}H,^{15}N] NMR at 298 K until completion after approximately 47 h. The final pH was determined to be 6.2.

Instrumentation. The NMR spectra were recorded on a Varian UNITY-INOVA-600 MHz spectrometer (^{1}H, 599.92 MHz; ^{15}N, 60.79 MHz). The ^{1}H NMR chemical shifts are internally referenced to TSP and the ^{15}N chemical shifts externally referenced to ^{15}NH$_4$Cl (1.0 M in 1.0 M HCl in 5% D$_2$O in H$_2$O). The ^{1}H spectra were acquired with water suppression using the WATERGATE sequence.[18] The two-dimensional [^{1}H,^{15}N] heteronuclear single-quantum coherence (HSQC) NMR spectra (decoupled by irradiation with the GARP-1 sequence during the acquisition) were recorded using the sequence of Stonehouse et al.[19] Details of the acquisition and processing parameters have been described previously.[11] The two-dimensional NOESY spectra of the unplatinated duplex was acquired with 80 transients over a ^{1}H spectral width of 12 kHz into 4096 data points for 768 t_1 increments using a mixing time of 150 ms and a pulse repetition delay of 2 s. The solvent signal was suppressed by use of a WATERGATE routine. All samples (including buffers, acids, etc.) were prepared so that there was a 5% D$_2$O/95% H$_2$O concentration (for deuterium lock but with minimal loss of signal as a result of deuterium exchange). Spectra were recorded at 298 K, and the sample was maintained at this temperature when not immersed in the NMR probe.

The pH of the solutions was measured on a Shindengen pH Boy-P2 (su19A) pH meter and calibrated against pH buffers of pH 6.9 and 4.0. The volume of 5.0 μL of the solution was placed on the electrode surface and the pH recorded. These aliquots were not returned to the bulk solution (as the electrode leaches Cl$^-$). Adjustments in pH were made using 0.04, 0.2, and 1.0 M HClO$_4$ in 5% D$_2$O in H$_2$O, or 0.04, 0.2, and 1.0 M NaOH in 5% D$_2$O in H$_2$O.

Data Analysis. The kinetic analysis of the reactions was undertaken by measuring peak volumes in the Pt−NH$_3$ regions of the [^{1}H,^{15}N] spectra using the Varian NMR software package and calculating the relative concentrations of the various species at each time point, as described previously.[11] All species, other than ^{15}N-**1**, gave rise to two NH$_3$ peaks for the nonequivalent {PtN$_3$Y} groups. In some cases, overlap between peaks was significant (e.g., the peak for the nonaquated {PtN$_3$Cl} group of the aquachloro species **2** is coincident with the peak for **1**),[14] but in these instances, it was only one of the pair of the peaks that was overlapped. Thus, reliable intensities were obtained by doubling the volume of the second (discrete) peak. Most species also gave rise to resolved peaks in the Pt−NH$_2$ region of the [^{1}H,^{15}N] spectra and comparison of the time dependent changes in the two regions was used to confirm the peak assignments.

The appropriate differential equations were integrated numerically, and rate constants determined by a nonlinear optimization procedure using the program SCIENTIST (Version 2.0, MicroMath, Inc.). The errors represent one standard deviation. In all cases, the data were fit using appropriate first and second-order rate equations.

The ^{1}H NMR resonances of the duplexes **I** and **II** prior to platination were assigned from a NOESY spectrum by using established assignment strategies for right-handed B-form DNA.[20]

HPLC and ESI Mass Spectrometry. The final products from the reactions of **1** with **I** and **II** were analyzed by HPLC.[21] The solutions were stored at 277 K for several months, then diluted with H$_2$O by a factor of 100 prior to injection onto the HPLC column. A 10-μL or 90-μL aliquot was loaded onto either a Phenomenex Aqua analytical (5 μm, 125 Å particle size, 4.6 × 250 mm) or semipreparative (5 μm, 125 Å particle size, 10 × 250 mm) column and eluted using a Waters 600 gradient pump system with a Waters 486 UV detector. Computer control was maintained with the Millennium 32 software suite provided by Waters. Elutions were performed with acetonitrile in 50 mM ammonium acetate buffer (pH 5.4) at flow rates of 1 (analytical) or 6 (preparative) mL min^{-1}. The gradient profile is included in the Supporting Information together with the elution profiles for the final products from the two reactions. The fractions were collected into clean

(17) Kallansrud, G.; Ward, B. *Anal. Biochem.* **1996**, *236*, 134−138.

(18) Piotto, M.; Saudek, V.; Sklenar, V. *J. Biomol. NMR.* **1992**, *2*, 661−665.
(19) Stonehouse, J.; Shaw, G. L.; Keeler, J.; Laue, E. D. *J. Magn. Reson. Ser. A* **1994**, *107*, 174−184.
(20) Wijmenga, S. S.; Mooren, M. M. W.; Hilbers, C. W. In *NMR of Macromolecules, A Practical Approach*; Roberts, G. C. K., Ed.; Oxford University Press: New York, 1993; pp 217−288.
(21) The HPLC and mass spectral analyses of the final adducts were undertaken with the sample from the NMR experiment for the reaction with **II** (^{15}N-**1**), whereas for the reaction with **I** the reaction was repeated under identical conditions to the NMR experiment, but using unlabeled **1**.

bottles and then extensively dialyzed for 24 h against cold water (277 K) to remove any salts. The samples were lyophilized and then stored frozen for several months prior to analysis by electrospray mass spectrometry (performed at The University of Arizona). The separated fractions were dissolved in 1 mL of H_2O/MeOH (1:5) with 5% NH_4-OH. Data were acquired in the negative mode with ESI source.

Reaction of 1 and I.[21] The HPLC elution profile (Figure S10) showed peaks for two major adducts with similar retention times (28.5 and 29 min). The two fractions were separated and the ESI mass spectra of both isolated conformers showed peaks attributable to a cross-linked adduct of **1** and the duplex (calcd molecular weight 8203.1 amu). For both fractions peaks from Na^+ adducts reduced the intensity of the drug−DNA adduct peaks but the 4-, 5-, 6-, and 7- charge states are clearly observed.

Reaction of ^{15}N-1 and II.[21] The HPLC elution profile (Figure S10) showed only one major adduct (retention time 28 min). The ESI mass spectrum of the isolated adduct is consistent with a cross-linked adduct of ^{15}N-**1** and the duplex (calcd. molecular weight 8213.1 amu) as the major species with peaks observed attributable to the 4-, 5-, 6-, 7-, and 8- charge states of the double stranded adduct.

For both 1,4 cross-linked conformers (and to a much lesser extent the 1,6 cross-link) peaks were also observed in the ESI mass spectra attributable to small amounts of both single-stranded adduct and unplatinated duplex (**I** or **II**). This could be indicative of some coelution of minor products (Figure S10), some conversion of the interstrand adducts to intrastrand adduct(s) over time, or to some decomposition of the double-strand adducts under the conditions of the ESI−MS procedure.

Molecular Modeling. Models depicting the electrostatic preassociation of **1** in the minor groove of 5′-d(ATAT**G**TACATAT)$_2$ (**I**) and 5′-d(TAT**G**TATACATA)$_2$ (**II**) were generated using HyperChem version 5.11. Computations were performed using a derivative of the AMBER parameter set and an all-atom force field developed by Yao et al.,[22−23] as described previously.[4] **1** was manually docked in the minor groove of **I** and **II** with the positioning of the linker based on the observed proton chemical shift changes in the first ^{1}H NMR spectra obtained immediately after addition of **1** to each sequence (see below). Small adjustments in the orientation of the $-CH_2-$ chains were made in order to direct the terminal platinum atoms toward the major groove. The system was relaxed between each of these iterations with 100 steps of molecular mechanics using a steepest descent algorithm. The final images were created in SwissPDBViewer v3.72 and rendered using POVRay v3.11 g.

Results

The platination reactions of the self-complementary 12-mer duplexes 5′-{d(ATAT**G**TACATAT)$_2$} (**I**) and 5′-{d(TAT**G**TATACATA)$_2$} (**II**) with ^{15}N-**1** were followed by [^{1}H,^{15}N] NMR spectroscopy. The methodology followed that reported previously[11] for the reaction of 1,1/t,t with duplex **I** and the conditions for the reactions (298 K, pH 5.3) were chosen to allow best comparison with the results of that study. At this pH the Pt−NH_3 signal of the monoaqua monochloro species **2** appears in a clear region of the spectrum allowing the concentration of this species to be monitored over time. As previously, the $^{15}NH_3$ signals for the {PtN_3X} (end) groups fell within a narrow range in the ^{15}N dimension (δ −60 to −64), but were well separated in the ^{1}H dimension, allowing identification of the Pt−NH_3 peaks of all the species involved in the reaction. In the $^{15}NH_2$ region, significant overlap was found, as well as suppression of some peaks in proximity to the ^1H_2O signal, rendering these signals less useful for the assignment of the different adducts. However, changes in the shifts of both the $^{15}NH_3$ and $^{15}NH_2$ signals of the {PtN_4} group of the linker proved useful in monitoring changes in electrostatic and/or H-bonding interactions of this group with the DNA. ^{1}H NMR spectra were also acquired to monitor oligonucleotide base-pairing through examination of the imino resonances and to verify Pt binding to GN7 by means of the shift of the H8 resonance from that of the unplatinated duplexes. The ^{1}H NMR resonances of the unplatinated duplexes (**I** and **II**) were assigned from NOESY data, allowing identification of specific changes that occurred immediately upon addition of ^{15}N-**1**.

Scheme 2. Interstrand Cross-linking of **1** with Duplexes **I** and **II**, According to Model 1

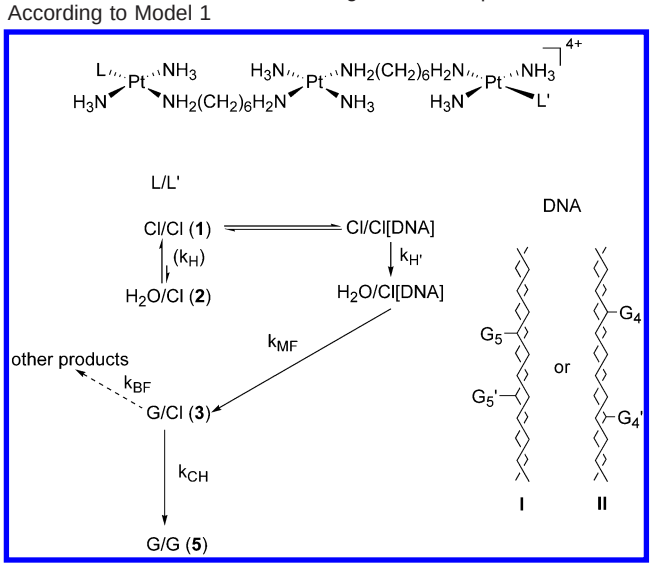

The DNA binding of bifunctional platinum drugs follows the stepwise sequence observed previously for 1,1/t,t[11] with evidence for noncovalent association through electrostatic interaction and hydrogen-bonding, aquation followed by monofunctional covalent binding and finally fixation of the interstrand cross-link through bifunctional binding (Scheme 2).

The chemical shifts of all intermediate and bifunctional product species observed during the reactions with **I** and **II** are summarized in Tables 1 and 2. Representative [^{1}H,^{15}N] HSQC spectra for the two reactions are shown in Figure 1 and plots showing changes in selected regions of the ^{1}H spectra for the two reactions are shown in Figures 2, 3, and 4.

Pre-covalent Binding Step. To examine the pre-covalent binding interactions of **1** with the polyanionic duplexes, [^{1}H,^{15}N] and ^{1}H spectra were recorded immediately after the start of the reaction. The change in chemical shifts compared to a control sample (no DNA added to ^{15}N-**1** in 15 mM phosphate buffer, pH 5.3) was used as an estimate for the strength of the electrostatic interaction between the platinum complex and the duplex.[24] Table 3 summarizes the changes in ^{1}H and ^{15}N shifts of the Pt-am(m)ine groups of ^{15}N-**1** on addition to duplexes **I**

(22) *HyperChem Computational Chemistry*, HyperChem, Release 5.11 ed.; HyperCube, Inc.: Gainesville, FL, 1995; pp 142−144, 151−152.
(23) Yao, S.; Plastaras, J. P.; Marzilli, L. G. *Inorg. Chem.* **1994**, *33*, 6061−6077.
(24) Since the reactions of ^{15}N-**1** with the two sequences were carried out with a slightly different excess of DNA present only the initial changes in ^{1}H,^{15}N shifts of the Pt−NH_2 and Pt−NH_3 groups are compared for both reactions, while the changes in chemical shift of peaks in the ^{1}H spectra of the two duplexes are discussed merely qualitatively.

Table 1. ^{1}H and ^{15}N Shifts for Intermediates Observed during the Reaction of 1,0,1/t,t,t (^{15}N-**1**) with the Self-Complementary Duplexes 5′-{d(ATAT**G**TACATAT)$_2$} (**I**) and 5′-{d(TAT**G**TATACATA)$_2$} (**II**) (pH 5.3)[a]

species	duplex	Pt–NH_3 end		Pt–NH_3 linker		Pt–NH_2 end		Pt–NH_2 linker	
1,0,1/t,t,t		δ ^{1}H	δ ^{15}N	δ ^{1}H	δ ^{15}N	δ ^{1}H	δ ^{15}N (trans ligand)	δ ^{1}H	δ ^{15}N
L,L′ = Cl (**1**)	**I**	3.91	−64.2	4.27	−63.3	5.05	−46.9 (Cl)	ca. 4.77−4.83[b]	ca. -43.9[b]
	II	3.89	−64.4	4.28	−62.8	5.01	−47.0 (Cl)	4.73	−44.2
		(3.86)	(−64.4)	(4.15)	(−63.7)	(5.03)	(−46.7)	(4.70)	(−44.0)
L = Cl, L′ = H_2O (**2**)[h]	**I**	*c*	*c*	*c*	*c*	*c*	(Cl)[c]	*e*	*e*
		4.19	−61.8			*d*	(OH_2)[d]		
	II	*c*	*c*	*c*	*c*	*c*	(Cl)[c]	*e*	*e*
		4.15	−61.9			*d*	(OH_2)[d]		
		(4.00)	(−62.5)						
L = N7G, L′ = Cl (**3**)	**I**	3.93	−64.2	4.28−4.29[f]	−63.3	*ca.* 5.05[g]	−46.9(Cl/N7G)	*e*	*e*
		4.29	−60.6			5.12	−46.9 (N7G/Cl)		
	II	3.93	−64.3	4.27	−63.7	*ca.* 5.01[g]	−47.0 (Cl/N7G))	4.83[i]	−44.3[i]
		4.31	−61.1			5.12	−47.2 (N7G/Cl)		

[a] ^{1}H referenced to TSP, ^{15}N referenced to $^{15}NH_4Cl$ (external), δ in ^{15}N dimension ± 0.2 ppm. ^{1}H and ^{15}N shifts for **1** and **2** in 15 mM phosphate buffer pH 5.3,in the absence of DNA are shown in parentheses. [b] The linker −NH_2 peak(s) are mostly eliminated due to proximity to ^1H_2O peak but some strongly deshielded resonances are observed. [c] Assumed to be concealed by peaks for **1**. [d] NH_2 peak for **2** expected at ca. 4.85/−61.0 at pH 5.3;[14] this is too close to H_2O to resolve at this concentration (ca. 40 μM). [e] Assumed to lie too close to H_2O to be visible. [f] Partially overlapped with **1**. [g] Measurement of peak volumes indicates that one or two of the four NH_2 protons of **3** are concealed by the peak for **1**. [h] The peak for **2** may also have a contribution from the aquated monofunctional adduct **4** (G/H_2O) as no distinct peak is observed for this species for either sequence. [i] The monofunctional adduct may also contribute to the peaks at δ 4.98/−44.3 and δ 4.73/−44.3 (see Figure 1b).

Table 2. ^{1}H and ^{15}N Shifts of the 1,4- and 1,6-GG Interstrand Adducts (**5**) Formed on Reaction with Duplex **I** and **II** (298 K)[a]

duplex		Pt–NH_3 δ ^{1}H/^{15}N end B_1/B_2	Pt–NH_3 δ ^{1}H/^{15}N end A_1/A_2	Pt–NH_3 δ ^{1}H/^{15}N linker	Pt–NH_2 δ ^{1}H/^{15}N end	Pt–NH_2 δ ^{1}H/^{15}N linker[c]
I	conformer **X**	4.37/−60.6	4.30/−60.9[d]	4.29/−63.5[d]	5.06−5.21/−47.4[b]	4.85/−43.9
	(major)	4.35/−60.9			5.16−5.46/−45.3[b]	4.91/−43.4
	conformer **Y**	4.37/−60.6	4.57/−59.7	4.35/−63.2[e]	5.06,5.26/−46.5[b]	4.91/−44.3
	(minor)	4.35/−60.9	4.51/−59.9	4.35/−63.2[e]		4.97/−44.3
II		4.37/−61.0	4.31/−61.0[d]	4.40/−63.1	*ca.* 5.01−5.26/−47.6[f,g]	4.98/−44.3
				4.31/−63.6	5.07, 5.26/−47.1[g]	4.87/−44.3
				4.28/−63.6	*ca.* 5.26−5.38/−45.3[f,g]	*ca.* 4.76/−44.3

[a] ^{1}H referenced to TSP, ^{15}N referenced to $^{15}NH_4Cl$ (external), δ in ^{15}N dimension ±0.2 ppm. [b] Peaks at δ ^{15}N −47.4 appear first and partially convert to other peaks with ^{15}N shifts at −45.3 and −46.5; peaks for conformers **5X** and **5Y** cannot be distinguished in this region. [c] For duplex **I** the linker −NH_2 peaks are mostly eliminated due to proximity to the ^1H_2O peak (δ 4.78) and only strongly deshielded peaks are seen; this is not the case for duplex **II**.[d] Very broad peak. [e] One sharp peak and one broad peak at similar ^{1}H/^{15}N shift. [f] Several merged peaks with similar ^{15}N shift. [g] Products with peaks at δ^{15}N −47.1 and −47.6 appear first and partially convert to final product conformers with ^{15}N shifts at δ^{15}N −47.1 and −45.3. In the final product the peaks at δ^{15}N −47.1 and −47.6 are merged and account for 89% of the total product and the peaks at δ^{15}N −45.3 for 11%.

Table 3. Changes in ^{1}H and ^{15}N Shifts of the Pt-am(m)ine Groups of ^{15}N-**1** on Addition to Duplex **I** and **II** (pH 5.3, 298 K)

	$\Delta\delta$ ^{1}H/^{15}N NH_3 (end)	NH_3 (linker)	NH_2 (end)	NH_2 (linker)
I + 1,1/t,t	0.05/0.3		0.02/0	
I + 1,0,1/t,t,t (**1**)	0.05/0.2	0.12/0.4	0.02/−0.2	0.07−0.13/0[a]
II + 1,0,1/t,t,t (**1**)	0.03/0	0.13/0.9	−0.02/−0.3	0.03/−0.2

[a] The linker −NH_2 peaks are mostly eliminated to due proximity to the suppressed H_2O peak, but some strongly deshielded resonances are seen (see Table 1 and Figure 1a).

and **II**. The results of 1,1/t,t with duplex **I**[11] are added for comparison. In all cases the interaction with the DNA results in a comparable deshielding in the ^{1}H dimension of the signals attributed to the NH_3 (end) groups in the {PtN_3Cl} moiety of ^{15}N-**1** and 1,1/t,t. For both sequences a more pronounced deshielding is detected for the linker (compared to the end) NH_3 groups in ^{15}N-**1**, as expected due to the higher charge (+2) of the central {PtN_4} unit. Noteworthy is the significant shift ($\Delta\delta$ = 0.9) in the ^{15}N dimension for the linker NH_3 groups in the presence of **II**, indicating a strong interaction with the duplex.

Differences in the interactions of the two sequences are also evident from the ^{1}H shifts of the CH_2 groups of the linker (Figure 4). For **1** in the absence of DNA there are three broadened multiplets at δ 1.38 (CH_2 3/4), δ 1.68 (CH_2 2/5), and δ 2.68 (CH_2 1/6): (numbering scheme: H_2N−Pt−NH_2-CH_2(1)CH_2(2)CH_2(3)CH_2(4)CH_2(5)CH_2(6)NH_2−Pt−Cl). Whereas only slight changes ($\Delta\delta \leq 0.02$) are observed on addition of **1** to duplex **I**, significant changes to the linker protons are seen for duplex **II**. Notably, the peak at δ 1.68 (CH_2 2/5) splits into two (δ = 1.68 and 1.63, see Figure 4b). The peak at δ 2.68 (CH_2 1/6) may also split into two new peaks but this assignment is ambiguous due to considerable overlap with sugar protons in this region. The peak at δ 1.38 (CH_2 3/4) does not alter significantly. This pattern of nonequivalence for the 2/5 (and 1/6) CH_2 groups is consistent with a strong interaction between the central {PtN_4} unit and the duplex and presumably it is the CH_2 groups 1 and 2 close to the central linker that are most affected.

For duplex **II**, minor groove binding of the linker of **1** is further supported by the changes in chemical shifts detected for the adenine H2 protons of A(8) (and most likely also A(6)) ($\delta\Delta$ 0.09) and also for the H1′ protons of T(7) ($\delta\Delta$ 0.05) and

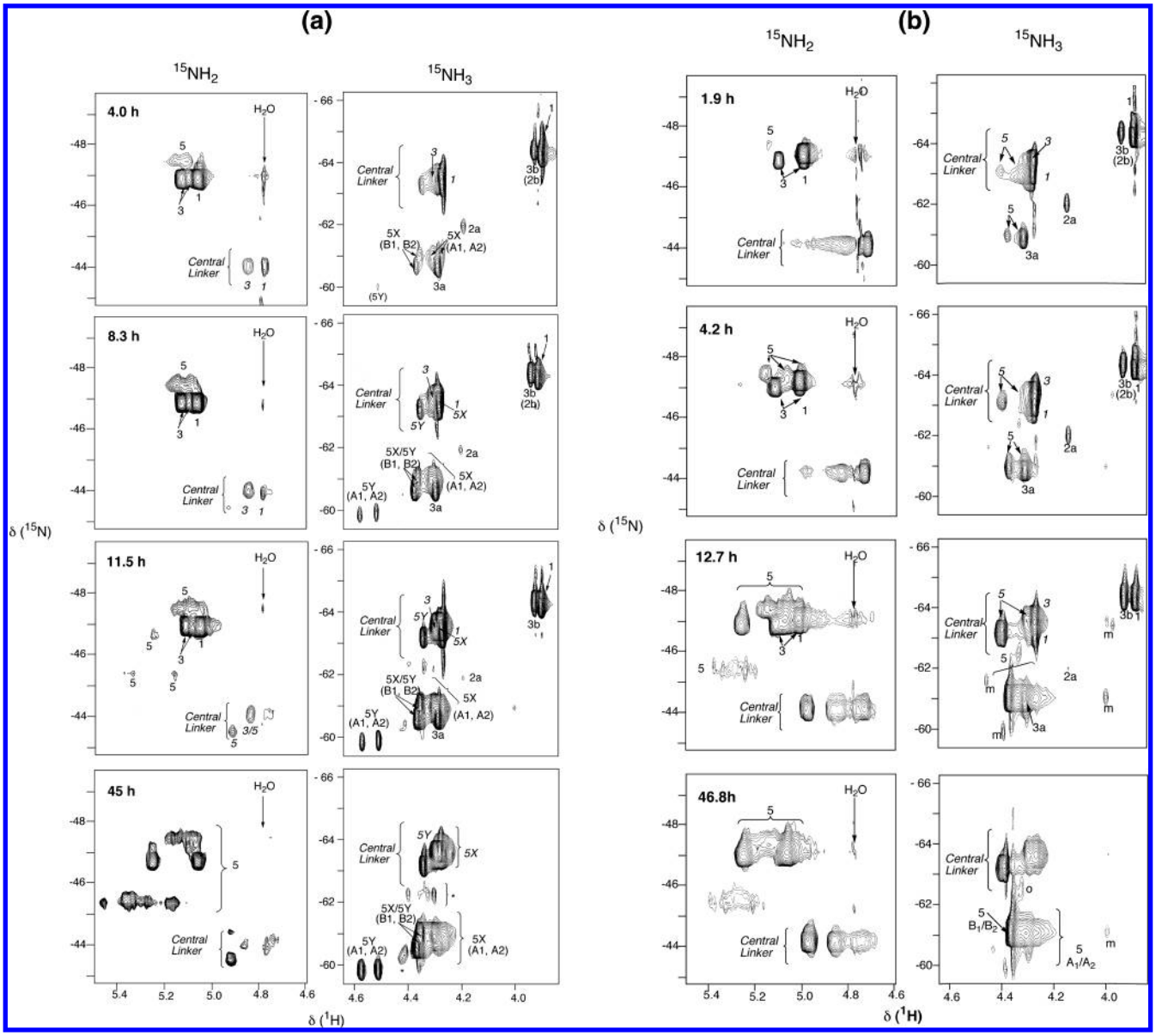

Figure 1. 2D [^{1}H,^{15}N] HSQC NMR (600 MHz) spectra at 298 K of (a) duplex **I** and (b) duplex **II** after reaction with ^{15}N-**1** for the times shown. Peaks are assigned to the Pt−NH_3 and Pt−NH_2 end and central linker groups in structures **1**−**5** in the pathway to formation of the 1,4- or 1,6 interstrand cross-linked adducts (see Scheme 1 and Tables 1 and 2). For duplex **I** there are two conformers of the bifunctional adduct **5X** and **5Y**. The assignments A_1/A_2 and B_1/B_2 correspond to the different NH_3 environments for the end groups (see text). Peaks for the individual conformers are not distinguishable in the Pt−NH_2 region but there are several different environments for the Pt−NH_2 groups as shown in the 45 h spectrum. In (a) peaks corresponding to the Pt−NH_2 groups of the central linker are mostly concealed by proximity to the H_2O peak for all species; peaks labeled * in the NH_3 region at δ −62.5 are assigned to other products. In (b) Peaks labeled "m" in the NH_3 region are assigned to other monofunctional adducts, (see text).

A(8) ($\delta\Delta$ −0.02). However, downfield shifts are found as well for the H6 proton of C(9) ($\delta\Delta$ 0.09) and the imino proton of one AT base pair, most likely T(5)A(8′) ($\delta\Delta = 0.07$, see Figure 3b). Minor changes ($\delta\Delta$ 0.02−0.03) are also observed for the methyl protons of T(3), T(6) and T(10).

For duplex **I**, minor groove binding is also supported by shifts in the nonexchangeable DNA protons but changes in the shifts are smaller due to the larger excess of DNA present. The largest changes are for the H2 proton of A(7) ($\delta\Delta$ 0.05) and the H1′ protons of T(2) and T(6) or T(10) ($\delta\Delta$ 0.03). These shifts did not occur when 1,1/t,t was added to the same duplex under identical conditions, further supporting that preassociation involves binding of the central linker in the minor groove. Significant shifts are also observed for several of the imino protons: the peak for the GC base-pair shifts very slightly downfield ($\delta\Delta$ 0.013) and the AT base-pair peaks T(4)−A(9′) and A(3)−T(10′) shift by +0.012 and −0.015, respectively. The central base-pair, T(6)−A(7′) is unchanged.

Aquation Step. In both reactions, the monoaqua monochloro species **2** accounts for approximately 3% of the total Pt−NH_3 species in the first [^{1}H,^{15}N] NMR spectrum (20 min), compared to 6% found for the control solution at the same time. All ^{1}H,^{15}N resonances of the {PtN_4} linker group as well as the signals for the {PtN_3Cl} moiety are assumed to be concealed by the signals of **1**. The Pt−NH_3 (end) resonance of the {PtN_3O} group shows a pronounced downfield shift ($\Delta\delta$ ^{1}H 0.15(**I**), 0.19 (**II**); ^{15}N 0.7) compared to the control sample, indicating a stronger electrostatic interaction with the duplex than for **1**, as a consequence of the increased charge (+2). The slight difference observed for the two sequences may not be significant as it

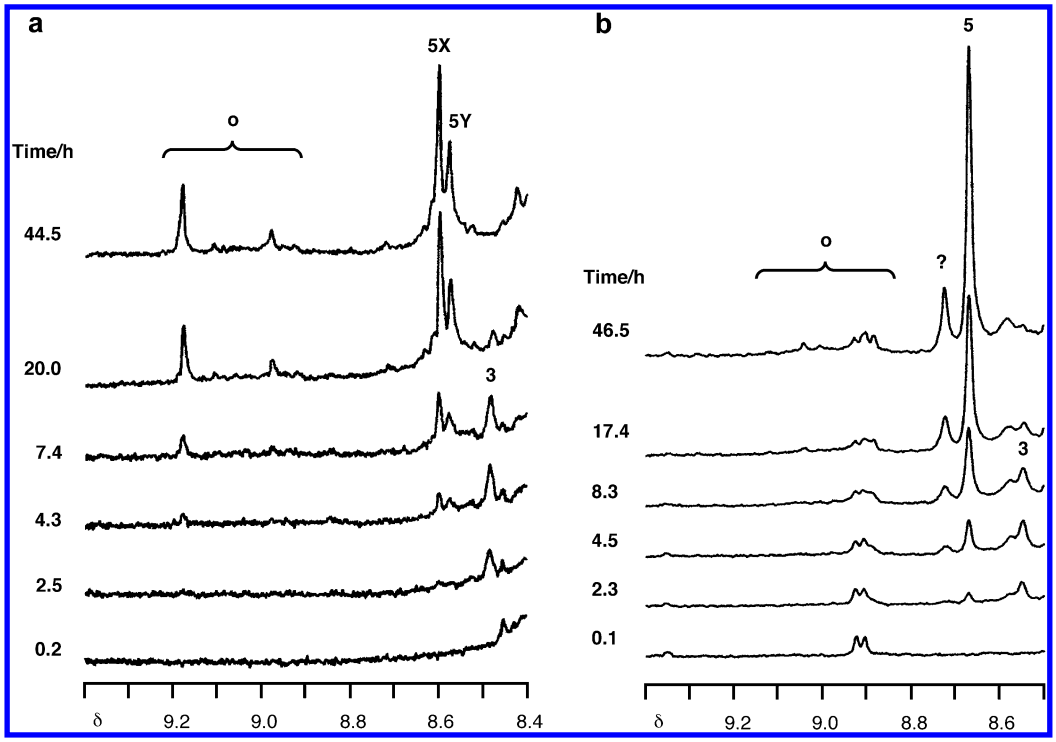

Figure 2. ^{1}H NMR spectra (600 MHz) of the aromatic regions of (a) duplex **I** and (b) duplex **II** after reaction with ^{15}N-**1** for between 0 and 47 h. In (a) the peaks are assigned to the H8 resonances of the G5 (and G5′) bases coordinated to platinum in the monofunctional adduct (**3**) and the two conformers (**X** and **Y**) of the 1,4-interstrand cross-link (**5**). In (b) the peaks are assigned to the H8 resonances of the G4 (and G4′) bases coordinated to platinum in the monofunctional adduct (**3**) and the 1,6-interstrand cross-link (**5**). The minor peak (at δ 8.73) is unassigned; it increases in intensity at a similar rate to the G H8 peak of **5** (δ 8.67) but curiously, there are no peaks in the [^{1}H,^{15}N] NMR spectra which correlate with this minor species. Peaks labeled "o" are assigned to other products (see text).

could occur if there was a very slight difference in pH for the two reactions.[14] The corresponding NH_2 (end) signal is not detected due to its close proximity to the H_2O peak. Similar behavior was observed previously for 1,1/t,t with duplex **I**.[11]

Monofunctional Binding Step. ^{1}H,^{15}N peaks for the monofunctional adduct **3** were observed slightly earlier for duplex **II** (17 min) than duplex **I** (25 min). The ^{1}H/^{15}N shifts for the Pt−$(NH_3)_2$ group at the unbound end (peak **3b**, Figure 1) are identical (δ 3.93/−64.2) in both reactions and shifted significantly compared to the noncovalently bound ^{15}N-**1** (Table 1). The ^{1}H/^{15}N shifts of the Pt−NH_3 group bound to guanine N7 (peak **3a**, Figure 1) are also very similar for duplex **I** (δ 4.29/−60.6) and duplex **II** (δ 4.31/−61.1). Similarly, the peak observed for the Pt−NH_2 (end) groups (δ 5.12/−47.1) is identical for the two monofunctional adducts formed by ^{15}N-**1** and also for that formed by 1,1/t,t with duplex **I**.[11] In each case, it appears that this peak has a contribution from two protons of the Pt−NH_2 group coordinated to guanine N7 and perhaps also one proton of the unbound Pt−NH_2 group. The signal of the remaining proton(s) is assumed to be obscured by overlap with the peak for the noncovalently bound compound.

The results indicate very similar environments for the different Pt−NH_3 and Pt−NH_2 groups for the guanine-N7 bound {PtN_4} and unbound {PtN_3Cl} ends of the monofunctional adducts and are not influenced by the presence of the central linker, or by changes in the nature of the sequence. In each case, there is evidence for similar electrostatic interactions between the uncoordinated {PtN_3Cl} group and the DNA and similar H-bonding interactions for the bound Pt−$(NH_3)_2$ groups.

In the aromatic region of the ^{1}H NMR spectrum (Figure 2) peaks at δ 8.48 (**I**) and δ 8.55 (**II**) are assignable to the H8 of the coordinated G residues of the monofunctional adducts (**3**), based on the time dependent profile which are similar to those observed for **3** in the [^{1}H,^{15}N] spectra.

Central Linker. The similarity in the ^{1}H/^{15}N shifts of the Pt−NH_3 groups of the central linker in the monofunctional adducts formed by ^{15}N-**1** with duplex **I** (4.28(9)/−63.3) and duplex **II** (4.27/−63.7) indicates similar environments for these groups. However, a major difference is that for duplex **II** this environment appears to be quite different to that present in the preassociation complex prior to the covalent binding, where the large change in ^{15}N shift ($\delta\Delta = 0.9$) is indicative of a strong interaction with the DNA (see Figures 1a and b). Further evidence for movement of the central linker group in the reaction with **II** is the change in shift of the ^{1}H resonances of the linker CH_2 (2/5) protons in the preassociated complex and monofunctional adduct ($\delta = 1.68, 1.63$ (**1**); 1.80, 1.76 ppm (**3**), see Figure 4b). In addition, the observation of a strongly deshielded and highly dispersed ^{1}H,^{15}N peak in the linker Pt−NH_2 region of the [^{1}H,^{15}N] NMR spectrum in the early stages of the reaction (Figure 1b) is consistent with movement of the linker group. For duplex **I** there is some evidence that the preassociation complex and monofunctional adduct have quite similar environments for the Pt−NH_2 linker groups, based on the observation of peaks with similar ^{1}H/^{15}N shifts at the early stages of the reaction (Figure 1a). However, the proximity to the suppressed water peak precludes a detailed analysis of the peaks in this region.

Bifunctional Adduct Formation. For both sequences ^{1}H,^{15}N peaks assignable to the interstrand cross-link were first visible after ca. 1 h. Closure of the 1,4-interstrand cross-link is complete at 45 h which is marginally faster than observed for the 1,6

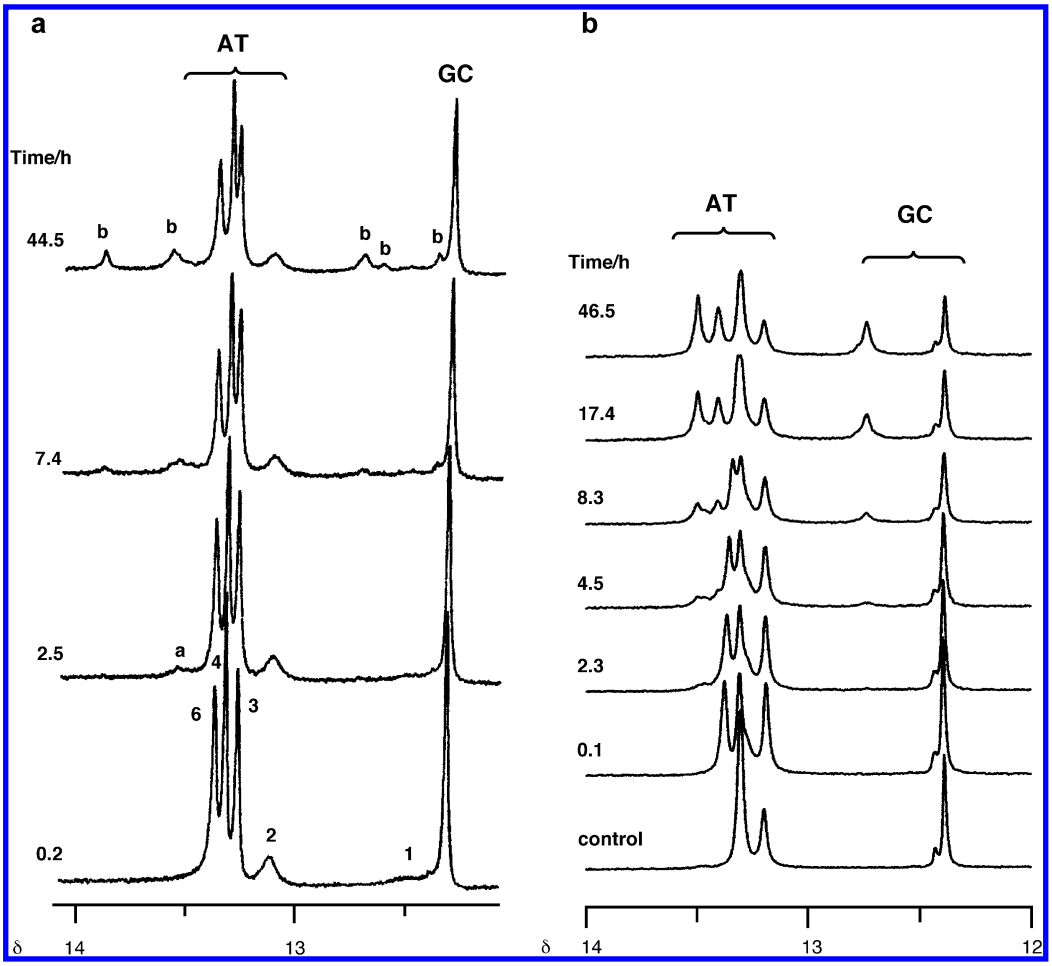

Figure 3. ^{1}H NMR spectra (600 MHz) of the imino regions of (a) duplex **I** and (b) duplex **II** after reaction with ^{15}N-**1** for between 0 and 45 h. In (a) assignments of resonances to base-pairs are indicated by numbers (5 = G(5)−C(8*), etc.), and letters indicate assignments to platinated adducts: a **3**; b **5**. In (b) the control spectrum shows the position of the imino protons before addition of ^{15}N-**1**. Pre-covalent binding association causes a selective shift for one of resonances of the AT base pairs (most likely T(5)A(8′) or T(3)A(10′)−see text). This peak reverts to its original position as the bound drug covalently attaches to the DNA to form the interstrand 1,6 interstrand cross-link (via the monofunctional adduct). Although the reactions are complete at 48 h intense signals for unplatinated duplex are present due to the excess of DNA used in the reactions. A greater excess of DNA was used in the reaction with duplex **I**.

cross-link (47 h) and also for 1,1/t,t with duplex **I** (48 h).[11] For the latter reaction, a small peak assignable to the monofunctional aquated species G/H_2O (**4**) was observed very close ($\delta\Delta$ ^{1}H 0.01) to the peak for the monoaqua monochloro species (**2**). No such peak was observed in the reactions of ^{15}N-**1** with either duplex **I** or **II**, indicating that either the species never achieves a concentration high enough to be detected (ca.10 μM) or the ^{1}H,^{15}N peak is coincident with that of the monoaqua monochloro species (**2**). Despite the similar profiles, analyses of the spectra reveal different behavior for the two sequences.

Formation of the 1,4-Interstrand Cross-Link. A significant difference between the formation of 1,4-interstrand cross-links by **1** and 1,1/t,t with duplex **I** is that in the latter the peaks are consistent with the presence of one predominant adduct.[11] In the present case, the appearance of peaks in the NH_3 (end) region is consistent with the presence of two distinct conformers of the 1,4 cross-link, which are present in a ratio of 2.6:1 (X:Y) (see below). These conformers are not interconvertible. Indeed heating results in splitting of the G(H8) resonance of the minor conformer **5Y** but the signals still do not coalesce with those of **5X** (see Figure S8 in Supporting Information).

Further evidence for two conformers is obtained from the ^{1}H NMR spectrum (Figure 2a) where two peaks of unequal intensity (at δ 8.60 and 8.58), which increase in intensity at similar rates, are assignable to H8 protons of the platinated G residues. In contrast, only a single GH8 resonance (δ 8.59) was observed for 1,4-cross-link formed by 1,1/t,t with the same sequence.[11] In the imino region (Figure 3a), there are two peaks of unequal intensity (δ 12.71 and 12.62) possibly assignable to GH1 in the two conformers (together with an additional peak at δ 12.37) whereas a single peak in this region (δ 12.75) was observed in the reaction with 1,1/t,t. There is one major pair of peaks assignable to the linker methylene groups 2 and 5 (δ 1.69 and 1.66), together with minor peaks in this region (δ 1.74, 1.59 and 1.85) that may be assignable to the methylene groups of the minor conformer (Figure 4a). Finally, two major adduct peaks with similar retention times are observed in the HPLC chromatogram of the final product (see Figure S10). In both cases the ESI mass spectrum of the isolated species is consistent with a cross-linked adduct of **1** and duplex **I**.

In the Pt-$^{15}NH_3$ (end) region of the [^{1}H,^{15}N] NMR spectrum (Figure 1a) the first sets of peaks assignable to the bifunctional adduct **5** are a broadened shoulder at δ 4.30/−60.9, slightly deshielded from the monofunctional G/Cl peak (**3a**) and two sharper more strongly deshielded peaks at δ 4.37/−60.6 and 4.35/−60.9. The broad peak has equal volume to the sum of

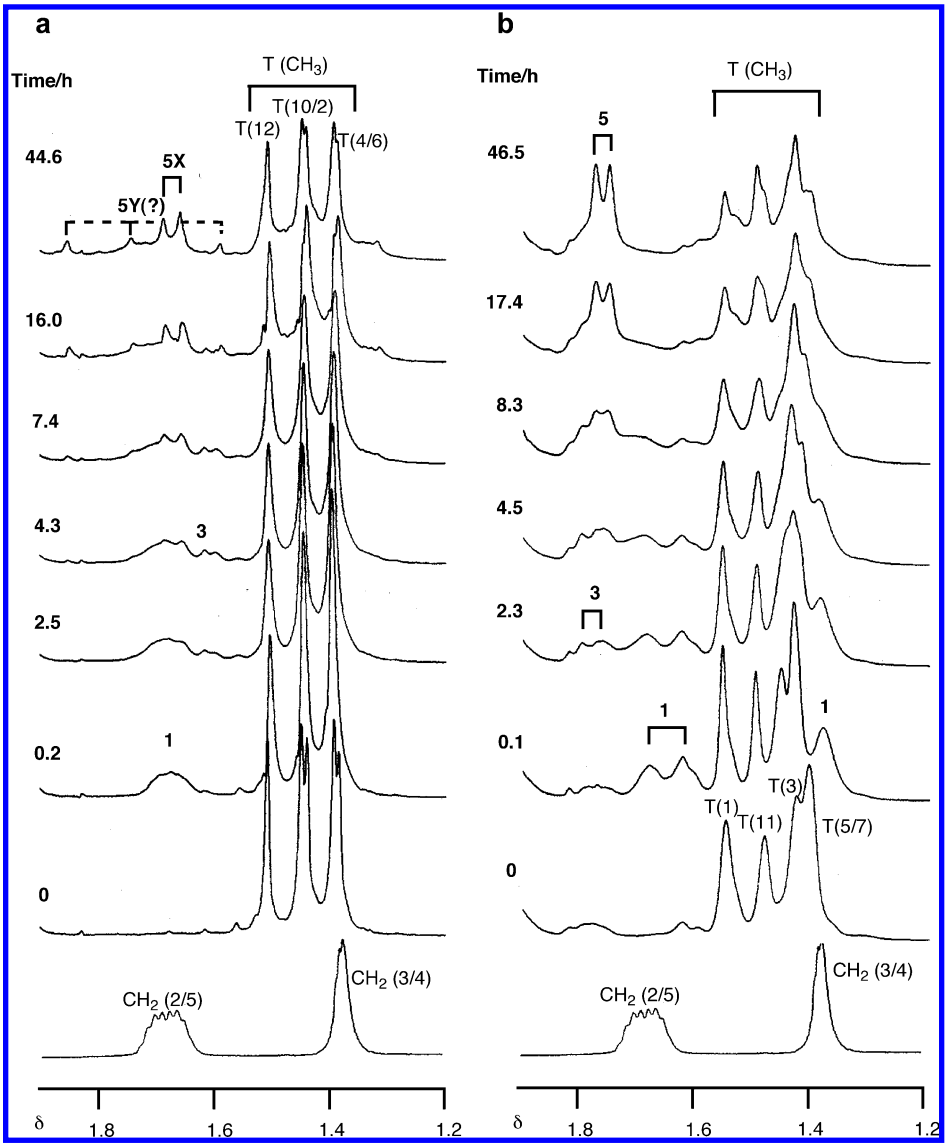

Figure 4. Comparison of the ^{1}H spectra following the formation of (a) 1,4- and (b) 1,6-interstrand cross-links by ^{15}N-**1** showing the region of the CH_2 protons of the linker. The bottom spectrum shows the ^{1}H spectrum of ^{15}N-**1** in 15 mM phosphate (pH 5.3) in the absence of DNA and the spectra at 0 h indicate the positions of the T-methyl protons in the two duplexes (**I**: 2.96 mM, **II**: 2.62 mM, in 15 mM phosphate, pH 5.3) before the addition of ^{15}N-**1** (1.60 or 1.90 mM). The labeled peaks correspond to the CH_2 protons of the linker in the monofunctional (**3**) and bifunctional (1,4 or 1,6) adducts (**5**). On addition of **1** to **I** there is little change in the chemical shift of the multiplet at δ 1.68 corresponding to the CH_2 (2 and 5) groups, whereas for duplex **II** pre-covalent binding association leads to nonequivalence of these groups and two peaks are observed (δ 1.68 and 1.63). Formation of the 1,4 cross-link gives rise to a major pair of peaks in this region (δ 1.69,1.66) as well as three minor peaks (δ 1.74, 1.59, and 1.85) which is possibly consistent with the formation of major (**5X**) and minor (**5Y**) conformers observed in the [^{1}H, ^{15}N] NMR spectra. On the other hand on formation of the 1,6 interstrand cross-link only one pair of peaks (δ 1.78 and 1.75) is observed assignable to the CH_2 groups 2 and 5 and these peaks are more strongly deshielded than for the 1,4 interstrand cross-link.

the two sharp peaks, while this latter pair of peaks share an identical time dependence. This pattern of peaks is very similar to that observed for the bifunctional adduct formed by 1,1/t,t with this sequence.[25] The spectrum can be interpreted in a similar manner by considering the schematic model of the 1,4-interstrand cross-link (below) developed in that case.[11,12] The sharp pair of peaks is assigned to the Pt−NH_3 environments B_1 and B_2 which are coordinated to different Pt atoms and are both hydrogen-bonded to a guanine O6. The broad peak is then assigned to the Pt−NH_3 A_1 and A_2 environments pointing toward the phosphate backbone

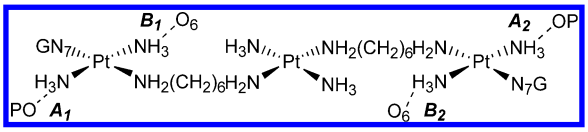

A pair of sharp, strongly deshielded peaks at δ 4.57/−59.7 and 4.51/−59.9 attributable to the minor conformer **Y** appear after ca. 3 h. On the basis of the time dependence and relative intensities of all the Pt−NH_3 peaks assignable to the bifunctional adduct, these peaks are assigned to the A_1 and A_2 groups. The B_1 and B_2 groups are assumed to be indistinguishable from those of the major conformer and contribute to the same two peaks

(25) The NMR structure of the 1,4-interstrand cross-link of **1** with the 8-mer 5′-$(ATGTACAT)_2$ (ref 31) shows an NOE cross-peak between G3′ NIH and the ammine protons of the Pt−$(NH_3)_2$ (end) group but no similar cross-peak is observed for G3 NIH. This difference is consistent with the observation here of two distinct ^{1}H/^{15}N peaks for the B_1 and B_2 Pt−NH_3 groups.

at δ 4.37/−60.6 and 4.35/−60.9. The time-dependence plots of the Pt−NH_3 peaks are provided in the Supporting Information. The strong deshielding of the Pt−NH_3 peaks for the minor conformer indicates that the Pt−NH_3 A groups are in strongly hydrogen bonded environments which are quite different from those of the major conformer. The average ratio of **X**:**Y** is 2.6:1 over the course of the reaction and when the reaction is complete conformer **X** accounts for 71% of the total 1,4-cross-link and **Y** for 29%.

In the Pt−NH_3 (linker) region assignment of peaks for the different conformers **5X** and **5Y** is ambiguous. The majority of the product gives rise to a very broad peak centered at δ 4.29/−63.5, not significantly removed from the peaks for **1** and **3**. A sharp peak significantly deshielded from this position appears at δ 4.35/−63.2 (a shift of 0.08 ppm in the ^{1}H dimension with respect to **1**), partly superimposed with a broad shoulder. The time dependence of both signals strongly suggests that they likely correspond to the Pt−NH_3 linker groups in conformer **Y** rather than conformer **X**. If the assignment is correct this means that for the minor conformer **Y** the protons of both the Pt−NH_3 groups of the linker are deshielded, indicative of more strongly hydrogen-bonded environments.

Formation of the 1,6-Interstrand Cross-Link. In contrast to the reaction of ^{15}N-**1** with duplex **I**, several pieces of evidence show the existence of only one major conformer of the 1,6-interstrand cross-link. The HPLC chromatogram of the final product shows only one major adduct peak (see Figure S10 in Supporting Information) and the ESI mass spectrum of the isolated adduct confirms this to be a cross-linked adduct of ^{15}N-**1** and the duplex. In the ^{1}H spectrum there is one major peak (at δ 8.67) assignable to the G H8 proton (Figure 2b) and only one peak (at δ 12.74) assignable to the G H1 imino proton of the bifunctional adduct (Figure 3b). Similarly, there is only one pair of peaks (δ 1.78, 1.75) assignable to the linker methylene groups 2 and 5 (Figure 4b). These peaks are more strongly deshielded than for the major conformer of the 1,4 cross-link (Figure 4a).

In the [^{1}H,^{15}N] HSQC spectra (Figure 1b), only one set of resonances is observed in the Pt−NH_3 (end) region. Two peaks of equal intensity are detected, similar to those observed on formation of the 1,4-GG interstrand cross-link by 1,1/t,t.[11] A sharp peak at δ 4.37/−61.0 and a very broad peak at δ 4.31/−61.0 are assigned to the Pt−NH_3 B and A groups, respectively (see above).

There are three distinct ^{1}H,^{15}N peaks assignable to the Pt−NH_3 groups in the central linker region of the 1,6-GG interstrand cross-link (Figure 1b): a strongly deshielded sharp peak at δ 4.40/−63.1 and two broader peaks at δ 4.31/−63.6 and δ 4.28/−63.6 with relative intensities of 2:1:1. A possible interpretation is that on formation of the bifunctional adduct one of the NH_3 groups of the central linker forms a hydrogen bond with the DNA leading to the pronounced downfield shift, while the other NH_3 group exists in two similar, but not identical, environments which are approximately equally populated. Consistent with this interpretation is a small change in the relative intensity of these two peaks with temperature and a change in line-shape of the sharp peak at 288 K consistent with two overlapped peaks (see Figure S7 in Supporting Information).

Minor Products. Similar to the reaction with 1,1/t,t some minor product species with ^{15}N shifts at ca. −62.5 ppm are formed in the reaction of ^{15}N-**1** with duplex **I**. These peaks start to appear after ca. 5 h, increase only slowly and have similar time dependence to two other minor peaks at δ 4.41 and 4.43/−60.4. The relative intensity and time dependent profiles of these minor peaks are similar to those of peaks that appear in the H8 region of the ^{1}H spectrum between 9.0 and 9.2 ppm (Figure 2a) and are assigned to other (cross-linked) adducts formed from **3**. These species represent ca. 10% of the final product. For the reaction with duplex **II** minor products with similar ^{1}H H8 and Pt−NH_3 ^{1}H/^{15}N shifts are also observed (Figure 1b and 2b) but account for only 3% of the total product. In this case the [^{1}H,^{15}N] HSQC NMR spectra also showed the presence of some minor peaks whose time dependent behavior was transient (see Figure 1b). In total these minor species never account for greater than 4% of the total species present. The peak at δ 4.00/−61.1 is consistent with a phosphato substituted species based on the chemical shift at the solution pH.[14]

Conformational Flexibility of the 1,4 and 1,6 Interstrand Cross-Links. In the study of the formation of the 1,4 interstrand cross-link by 1,1/t,t, time dependent changes in the Pt−NH_2 region of the [^{1}H,^{15}N] NMR spectrum showed that the initially formed bifunctional adduct converted irreversibly into other final product conformers via a series of sequential changes.[11] A similar behavior is observed here for both the 1,4- and 1,6-GG interstrand cross-links. In both cases ^{1}H,^{15}N peaks assignable to the bifunctional adducts were first visible in the Pt−NH_2 (end) region at the same time as they appeared in the NH_3 region (ca., 1 h). These initial peaks are almost identical for the two sequences (**I**, δ 5.15/−47.4 and 5.09/−47.4; **II**, δ 5.16/−47.6 and 5.07/−47.6) and are very similar to the ^{1}H/^{15}N signals of the monofunctional adducts (see Figure 1).

A major difference for the two sequences is in the timing of the appearance of new peaks in the NH_2 (end) region. For duplex **I**, peaks at two distinct ^{15}N shifts (δ −46.5 and −45.3) both start to appear after ca. 7.5 h. There are two distinct peaks of similar intensity at δ −46.5 with very different ^{1}H shifts (δ 5.26 and 5.06), whereas there is a single merged peak at δ −45.3 which covers a wide chemical shift range in the ^{1}H dimension (δ 5.16 to 5.46). The final intensity ratio of peaks at the three ^{15}N shifts is δ −47.4 (27%), δ −46.5 (32%), δ −45.3 (41%) (see Figure 1a). The peak distribution is comparable to that of the final product conformers of the 1,4 interstrand cross-link formed by 1,1/t,t with the same sequence: δ −47.5 (22%), δ −48.4 (46%), δ −45.5 (31%).[11] These similarities show that ^{1}H,^{15}N peaks for the Pt−NH_2 (end) groups for the individual conformers (**5X** and **5Y**) cannot be distinguished.

For formation of the 1,6 cross-linked adduct of ^{15}N-**1** new peaks in the NH_2 (end) region appear much earlier. Two peaks centered at δ −47.1 (δ ^{1}H 5.07 and 5.26) are first visible after 4 h (Figure 1b). Additional peaks centered at δ −45.3 (δ ^{1}H 5.26 and 5.38) are detected after approximately 8.5 h and resembled the signals that appeared at the same ^{15}N shift in the reaction with duplex **I**. By the end of the reaction, merged peaks at δ −47 account for 89% of the total product peaks with merged peaks at δ −45.3 accounting for the remaining 11%.

These profiles suggest that on formation of both the 1,4- and 1,6-interstrand adducts kinetically preferred conformers are formed in which the Pt−NH_2 (end) groups are in solvent exposed environments similar to those of the preassociated compound and the monofunctional adducts. These initially

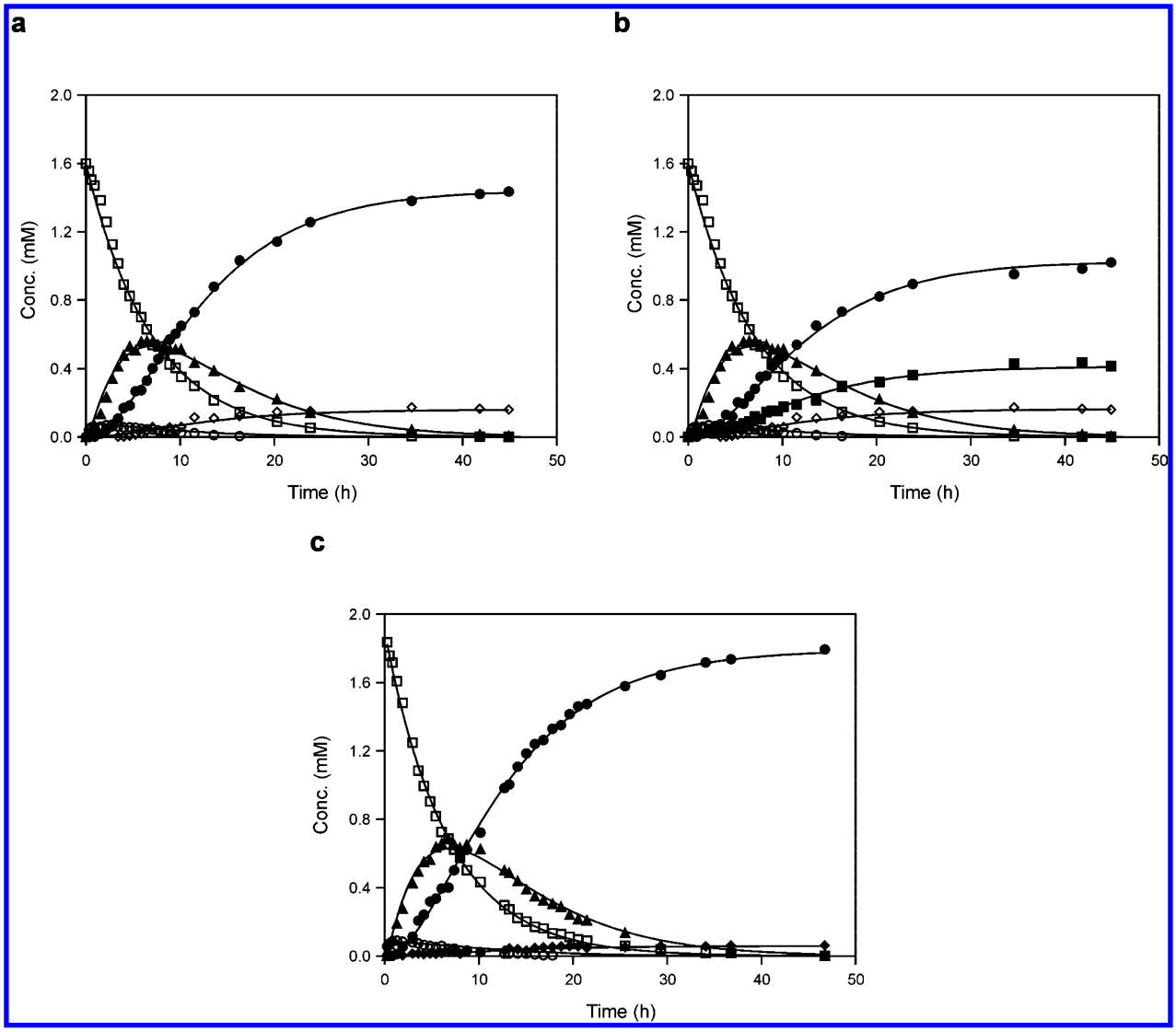

Figure 5. Plots of the relative concentration of species observed during formation of (a, b) 1,4- and (c) 1,6- interstrand cross-links by reaction (at 298 K) of ^{15}N-**1** with duplex **I** and **II**. The concentrations are based on the relative peak volumes of peaks in the Pt−NH_3 region. The curves are computer best fits for the rate constants shown in Table 4. Labels: **1** open squares, **2** open circles, **3** triangles, **5** filled circles, other products diamonds. (b) shows the formation of the major (**5X**, filled circles) and minor (**5Y**, filled squares) conformers of the 1,4-interstrand cross-link which are shown as combined product in (a).

formed products slowly transform into a variety of thermodynamically preferred conformers of the bifunctional adducts with several distinct environments for the NH_2 groups. The strong deshielding in the ^{1}H dimension for some of these environments suggests H-bonding interactions between the NH_2 protons and the DNA. The conformational change appears to occur faster for the 1,6- compared to the 1,4-interstrand cross-link and leads to final product conformers with less varied NH_2 environments.

Kinetic Analysis. The kinetic profiles for formation of the 1,4- and 1,6-interstrand cross-links are very similar (see Figure 5). For both sequences the monofunctional adduct (**3**) reaches a maximum concentration after ca. 7 h (32% and 35% of the total Pt for **I** and **II**, respectively). For the purposes of the kinetic fits the concentration of species present at each time point were obtained from the relative volumes of peaks in the Pt−NH_3 (end) region, as described previously for the reaction of 1,1/t,t with duplex **I**.[11] To allow comparison of the formation of the 1,4- and 1,6-interstrand cross-links the reactions of ^{15}N-**1** with duplexes **I** and **II** were analyzed by the same kinetic model (Model 1) as shown in Scheme 2. The reaction with duplex **I** was also modeled by a second kinetic model (Model 2) as defined in Scheme 3, in which the final product is treated as two separate conformers **5X** and **5Y**.

Scheme 3. Interstrand Cross-linking of **1** with Duplex **I**, According to Model 2

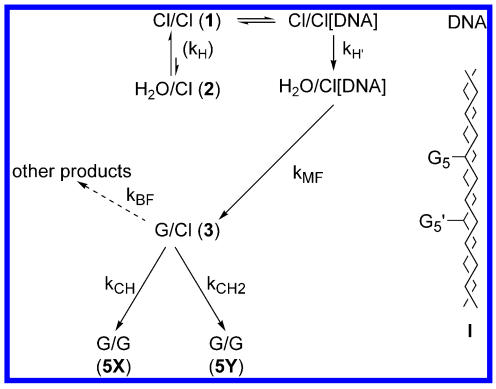

In each case, the pre-covalent binding association of **1** and **2** with the duplex (**I** or **II**) was not considered and both species were treated as unbound. The aquation process was modeled

Table 4. Rate Constants for the Reactions between **1** and Duplex **I** and **II**[a,b]

	1,0,1/t,t,t (**1**)			1,1/t,t[d]
rate constant	duplex **II** (model 1)	duplex **I** (model 1)	duplex **I** (model 2)[c]	duplex **I**
$k_{H'}/10^{-5}$ s^{-1}	4.17 ± 0.03	3.94 ± 0.03	3.93 ± 0.04	4.15 ± 0.04
k_{MF}/M^{-1} s^{-1}	0.34 ± 0.02	0.25 ± 0.02	0.24 ± 0.02	0.47 ± 0.06
$k_{CH}/10^{-5}$ s^{-1}	4.32 ± 0.04	4.21 ± 0.06	3.00 ± 0.05	3.39 ± 0.04
$k_{CH2}/10^{-5}$ s^{-1} [c]			1.21 ± 0.03	

[a] The rate constants are defined in Scheme 2 (Model 1) and Scheme 3 (Model 2). [b] Both reactions saw the formation of small amounts of other species (see text); in the reaction with duplex **II** some of these were clearly transient and were summed and treated as a monofunctional adduct that converted into the major product. In both reactions other species observed at the completion of the reaction were summed as "other products". The rate constants (k_{BF}, Scheme 2) obtained are meaningless in themselves and are not included here, but were used to ensure that the contributions of these species to the total concentration was taken into account when determining the rate constants for the formation of the major monofunctional and product species. [c] The reaction between **1** and duplex **I** affords two conformers of the 1,4 interstrand adduct, the rate constant k_{CH2} relates to the formation of the less abundant of these conformers from the monofunctional adduct, in that case k_{CH} relates to the formation of the major conformer. [d] Data from reference 11.

as an irreversible pseudo-first-order reaction. In the absence of a nucleophile, the aquation of **1** occurs such that the equilibrium between aquated and chloro species lies strongly toward the chloro side.[14] Factors such as reduced chloride ion concentration and/or altered aquation rates in the presence of DNA[13] affects this equilibrium and, once formed, the aqua chloro species (**2**) reacts rapidly and irreversibly with the duplex. Binding of **2** to duplex **I** or **II** was treated as an irreversible second-order reaction, first order with respect to the concentration of both **2** and duplex, respectively. Because no ^{1}H,^{15}N peak was observed assignable to a monofunctional aqua species (**4**) the formation of the bifunctional 1,4 or 1,6-cross-links (**5**) were modeled to form directly from the monofunctional adducts. These processes were treated as irreversible first order with respect to the concentration of **3**. In both cases, the minor products (peaks at δ ^{15}N −60.5) were summed together and for the purposes of the kinetic fits were assumed to form from the monofunctional adduct **3** by an irreversible first-order process. For the reaction with **II** the minor transient species (which may include derivatives of **1** in which a chloro ligand has been displaced by a phosphato ligand, see above) were summed together and were treated as a monofunctional adduct that converted into the major product. The rate constants obtained from the two kinetic models are listed in Table 4 and the computer best fits for the rate constants are shown in Figure 5.

The pseudo-first-order rate constant for the aquation process was found to have a slight sequence dependence, with a marginally higher rate constant obtained in the reaction with duplex **II**. The rate of monofunctional binding follows the same trend—the rate constant for binding of **2** to duplex **II** is approximately 30% higher than that to duplex **I** (independent of the model applied). As a consequence less of the aquated species (**2**) is seen in the reaction with duplex **II**, as it is consumed more rapidly. The monofunctional binding rate constant for **1** with duplex **I** is approximately one-half that found for the reaction with 1,1/t,t.[11] To verify this observation, the rate constants for the reaction between 1,1/t,t and **I** were fixed and applied to the data from the reaction between **1** and **I**. The overall reaction completion time remained the same but the time dependent profiles for the monofunctional (**3**) and bifunctional (**5**) adducts differed. The rate constants for the conversion of the monofunctional adducts (**3**) to the 1,4- or 1,6-interstrand cross-links were the same (within experimental uncertainties) for binding of **1** on the two different sequences. This result may be rationalized if aquation of the monofunctional adduct occurs prior to fixation of the cross-link and this step is rate limiting.

Discussion

The results presented here show that preassociation of a drug to DNA can be examined by use of the [^{1}H,^{15}N] NMR technique. For cisplatin, preassociation with single-stranded and double-stranded DNA has recently been studied by quartz crystal microbalance (QCM) techniques[26] and ESI−MS has also been used for $[Pt(NH_3)_4]^{2+}$−oligonucleotide interactions.[27] Our results show the importance of the preassociation step not only in affecting reaction kinetics but also the nature of the cross-links formed.

Kinetics of Formation of Interstrand Cross-Links. The first objective of this study was a comparison of the kinetics of formation of 1,4-interstrand cross-links by 1,1/t,t and 1,0,1/t,t,t with the same DNA sequence. The overall rate of formation is quite similar for the two reactions, occurring slightly faster in the case of 1,0,1/t,t,t. However, comparison of the individual steps of the reaction reveals some differences (Table 4). The aquation rate constant of 1,0,1/t,t,t in the presence of **I** is marginally lower than was found for 1,1/t,t (Table 4). A notable difference for the two reactions is the rate constant for monofunctional adduct formation which is 2-fold higher in the case of 1,1/t,t. A possible explanation is the strong pre-assocation in the minor groove for 1,0,1/t,t,t alters the approach to the N7 of the guanine in the major groove (see below and Figure 6).

Preassociation certainly has a strong influence on the aquation step. The pseudo-first-order rate constant for the aquation of ^{15}N-**1** in the presence of duplex **I** (or **II**) is approximately 40% of the value obtained for the forward (aquation) rate constant of **1** in 15 mM perchlorate or phosphate ($\sim 11 \times 10^{-5}$ s^{-1}) at the same temperature and pH.[14] A similar lowering of the aquation rate constant in the presence of duplex **I** is assumed to occur for 1,1/t,t.[11] The aquation rate constant for cisplatin is lowered in the presence of oligonucleotides[28] and we proposed previously[11,28] that the lowering of the aquation rate constant of Pt drugs may be a consequence of preassociation between the Pt complex and the DNA, restricting access of the solvent to the Pt coordination sphere and hindering formation of the five-membered transition state necessary for substitution (aquation) reactions. This suggestion is supported further from recent new evidence that the aquation of 1,1/t,t is faster by a factor of 1.4 in the presence of the single stranded 14-mer sequence 5′-d(ATACATGGTACATA)-3′, compared to the duplex with its complementary strand.[13]

The second objective of this study was a comparison of the stepwise formation of 1,4- and 1,6 interstrand cross-links by 1,0,1/t,t,t. Previous kinetic studies using gel electrophoresis have shown that 1,6-interstrand cross-links form significantly more slowly than 1,4-interstrand cross-links.[6] Our study shows a very

(26) Wang, Y.; Farrell, N.; Burgess, J. D. *J. Am. Chem. Soc.* **2001**, *123*, 5576−5577.
(27) Carte, N.; Legendre, F.; Leize, E.; Potier, N.; Reeder, F.; Chottard, J. C.; Van Dorsselaer, A. *Anal. Biochem.* **2000**, *284*, 77−86.
(28) Davies, M. S.; Berners-Price, S. J.; Hambley, T. W. *Inorg. Chem.* **2000**, *39*, 5603−5613.

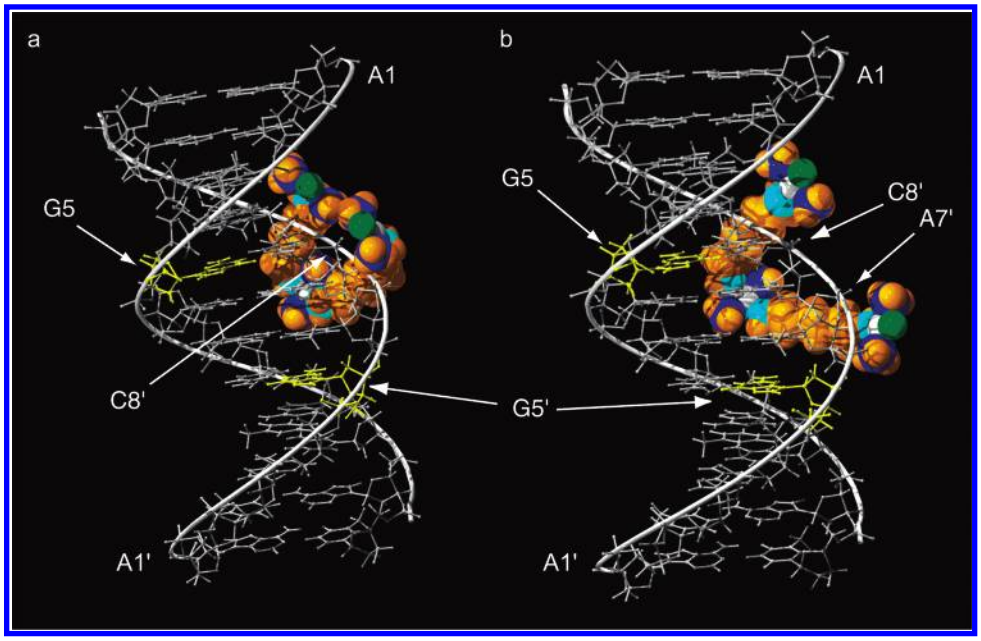

Figure 6. Molecular models illustrating the preassociation of **1** with duplex **I**. The {PtN_4} linker group remains anchored in the minor groove and the 1,4- interstrand cross-link between N7 platinated guanines can be formed by two distinct pathways consistent with the formation of two distinct conformers (5**X** and 5**Y**). In (a) the two $-(CH_2)_6-$ chains of **1** pass on either side of the C8′ phosphate, whereas in (b) there are two phosphate groups (C8′ and A7′) between the two $-(CH_2)_6-$ chains. The two guanine residues are shown in yellow, platinum in white, am(m)ine blue (pale and dark) and chloride in green.

different trend with very similar profiles for the two reactions (Figure 5). The different results may be partly a function of how the reactions are carried out. The gel electrophoresis study[6] involved prior formation of the monofunctional adducts on the single strands; the kinetics of interstrand cross-linking was monitored following addition of the complementary strands.

Role of Preassociation in Dictating the Nature of Interstrand Cross-Links. Our NMR studies show that the extent of preassociation with the DNA is significantly greater for 1,0,1/t,t,t than 1,1/t,t. This is not unexpected due to the higher charge of the trinuclear compound. The charge and hydrogen-bonding capacity of the central "noncovalent" tetraamine platinum is likely to contribute to the observed sequence specificity. Examination of the chemical shifts in the initial ^{1}H NMR spectra indicates that principal contacts are likely to be between the central linker group and the minor groove for both duplex **I** and **II**. Recently, 2-D NMR spectroscopy has been used to study the interactions with oligonucleotide duplexes of noncovalent dinuclear and trinuclear compounds containing 4,4′-dipyrazolylmethane (dpzm) as bridging ligand.[29] Unequivocal evidence for preassociation in the minor groove was observed. Even the simple cation $[Pt(en)_2]^{2+}$ has been shown to associate in the minor groove of DNA.[30]

The accumulated evidence from this work is that the preassociation dictates the nature and structure of the cross-links formed. For duplex **I** it is likely that the central linker group of 1,0,1/t,t,t remains in the minor groove on formation of both the monofunctional adduct and the final 1,4-interstrand cross-link. This interpretation is based on the NMR evidence described above, and is reinforced by the recently published structure of the 1,4 interstrand adduct of 1,0,1/t,t,t with the shorter 8-mer sequence 5′-{d(ATGTACAT)$_2$}[31] NOE contacts were shown between the NH_3 groups of the central linker and the T4′N3H (corresponding to T6 of duplex **I**) as well as between the linker CH_2 (6) to T4H1′, from the CH_2 (3′, 4′) to T2H1′ and from the CH_2 (3, 4) to A7H2. As the sugar H1′ protons and H2 proton of the adenine base are located in the minor groove of DNA, the NOE data again suggest that the linker is located in or close to the minor groove.

Given that the central linker is absent for 1,1/t,t it is reasonable to speculate that this preassociation of the central linker in the minor groove is responsible for the observation of two distinct conformers of the 1,4-interstrand cross-link for 1,0,1/t,t,t whereas only one (conformationally flexible) adduct was seen for 1,1/t,t. To investigate this possibility, we constructed molecular models for the preassociation of 1,0,1/t,t,t with duplex **I** in which the positioning of the central linker in the minor groove is based on the observed changes in chemical shift of the specific DNA ^{1}H resonances (see above). Models based on B-form DNA are not strictly valid representations of the final 1,4-interstrand cross-link as the NMR structure provides evidence for syn orientations for several of the bases in the bifunctional adduct.[31] However the B-form models are useful to visualize this first preassociation step and the pathways to covalent binding. The molecular models shown in Figure 6 demonstrate the feasibility of having the central linker remain within the minor groove while the {PtN_3Cl} end groups approach the N7 of the guanines in the major groove. This approach is made by interleaving the two $-(CH_2)_6-$ chains between the phosphate groups of the backbone. These models indicate two possible pathways for this to occur, based on the B-form geometry and the distance between the {PtN_3Cl} groups. In the first model, we consider (Figure 6a) one "arm" of **1** passes on the 3′ side of the C8′ phosphate while the other reaches around on the 3′ side of the A7′ phosphate. In the second model (Figure 6b), the second arm stretches to wrap around on the 3′ side of the T6′ phosphate so that there are two phosphate groups between the two arms. Both

(29) Wheate, N. J.; Collins, J. G. *J. Inorg. Biochem.* **2000**, *78*, 313−320.
(30) Franklin, C. A.; Fry, J. V.; Collins, J. G. *Inorg. Chem.* **1996**, *35*, 7541−7545.
(31) Qu, Y.; Scarsdale, N. J.; Tran, M.-C.; Farrell, N. *J. Biol. Inorg. Chem.* **2002**, *8*, 19−28.

of these structures come close to presenting Pt to the N7 of guanine and only slight distortion from the B-form DNA structure (which is known to occur)[31] would allow covalent binding without the need for the linker to move from the minor groove. The fact the two conformers can be separated on an HPLC column infers quite different global structures, consistent with these models.

Consideration of the molecular model for preassociation of 1,0,1/t,t,t with duplex **II** (Figure S11, Supporting Information) demonstrates an interesting difference. To achieve platination of the two guanine residues the distance is simply too far if the central linker remains in the initial position in the minor groove and the 1,0,1/t,t,t must "diffuse" off the DNA for covalent binding to occur. We see clear evidence for this movement of the linker from changes in chemical shifts of certain CH_2 linker protons and the linker as well as the $Pt-NH_2$ and $Pt-NH_3$ groups at the monofunctional binding step.

Structures and Conformational Flexibility of the Interstrand Cross-links. Our results predict subtle but significant differences in structures for the 1,4- and 1,6-interstrand cross-links of **1** that may lead to differential protein recognition and "downstream" effects. It is notable that for the 1,6- interstrand cross-link the ammine and amine protons of the central linker as well as (some of) the linker methylene protons appear to exist in environments that are H-bonded to the DNA. These strong deshielded resonances were not observed for the (major) 1,4- interstrand adduct.

The 1,4 cross-link of **1,** which spans four base-pairs, covalently binds to guanine N7 and binds simultaneously to both the minor and major grooves has some characteristics in common with each of two distinct types of DNA threading agents: the netroposin-amsacrine hybrid NetAmsa[32] and the pluramycin antitumor antibiotic Altromycin B.[33] For NetAmsa the netroposin tail spans four base-pairs in the minor groove and long residence times are achieved through the threading intercalation. In the case of **1**, long residence times are achieved from covalent binding to guanine N7 and in this aspect of the binding there are similarities with Altromycin B. The altromycins intercalate through the DNA molecule via a threading mechanism, which places saccharide groups in the minor and major groove. These steering interactions place the reactive epoxide group in the major groove allowing electrophilic attack on guanine N7.[33] Nevertheless, there are clear differences in the mode of the groove to groove cross-linking for **1** and for threading intercalators. The charged central $\{PtN_4\}$ linker is anchored in the minor groove and the $-CH_2-$ chains must wrap around the helix to achieve binding to the guanine N7 in the major groove. This novel mechanism for sequence recognition and binding may be an important aspect of the different antitumor activities of **1** and dinuclear analogues that lack the charged central linker.

The NMR structure of the 1,4 interstrand cross-link formed by 1,0,1/t,t,t with the self-complementary alternating purine-pyrimidine 8-mer 5′-$\{d(ATGTACAT)_2\}$ shows delocalized distortions beyond the binding site, specifically the induction of the syn conformation on the adenines.[31] Similar structural changes are indicated[12] for the 1,4 interstrand G(8)G(18) cross-link formed by 1,1/t,t with the 14-mer duplex 5′-d(ATACATG-(7)G(8)TACATA)-3′·5′-d(TATG(25)TACCATG(18)TAT)-3′ and there is a significant distortion of the 5′T residue adjacent to the platinated G, consistent with the findings from use of chemical probes to investigate the conformation of interstrand cross-links formed by 1,0,1/t,t,t.[6] Both di- and tri-nuclear Pt compounds of this class induce an irreversible B → Z conformational change in poly(dG-dC)·poly(dG-dC).[34] Duplexes **I** and **II** were both chosen for their alternating purine-pyrimidine sequence, a necessary requirement for the left-handed Z-DNA conformation. A notable feature of the reaction of 1,1/t,t with duplex **I** was the gradual and irreversible transformation of peaks in the $Pt-NH_2$ region, from an initially formed conformer(s) to product conformer(s).[11] The present study shows that these transformations are a common feature observed also for both the 1,4- and 1−6-interstrand cross-links of 1,0,1/t,t,t. For the initially formed adducts, the $^1H/^{15}N$ shifts of the $Pt-NH_2$ (end) groups are similar to those of the preassociated complex and the monofunctional adduct and indicate environments where the NH_2 protons have no contacts except with solvent. For the final product conformer(s) there are a range of distinct NH_2 environments indicative of interactions between the NH_2 protons and the DNA as a result of a changes in the DNA conformation. The similarity in the results for the three different studies suggest that the changes in the shifts of these $Pt-NH_2$ protons could be a useful indicator of the induction of the syn conformation on bases beyond the binding site. It is of interest to investigate whether similar behavior occurs for related duplexes, which do not have alternating purine−pyrimidine sequences. In the study[12] of formation of the 1,4 interstrand G(8)G(18) cross-link by 1,1/t,t with the 14-mer duplex 5′-d(ATACATG(7)G(8)TACATA)-3′·5′-d(TATG(25)TACCATG(18)TAT)-3′ there was evidence for propagation of structural changes within the alternating purine-pyrimidine region of the sequence G(8)·C(22) to A(14)·T(15) and a possible B/Z junction where the sequence is broken at G(7)·C(22). In this case also there were gradual changes in the $^1H,^{15}N$ resonances in the $Pt-NH_2$ (end) region over time, but these changes were different to those observed here with duplexes **I** and **II**.

Long-range interstrand cross-links formed by 1,0,1/t,t,t bend DNA but are not recognized by HMG-domain proteins.[6] A structural feature deduced for the recognition of cisplatin-bound DNA by HMG proteins is intercalation of a phenylalanine moiety into the minor groove closest to the platinated site.[35] The presence of a third noncovalent Pt coordination unit, or even a diamine linker may inhibit this intercalation, thus providing a molecular rationale to the failure of HMG proteins to recognize these cross-links. An important result is that the long-range cross-links are, further, poor substrates for nucleotide excision repair.[6] This fundamental process is not only correlated with general cytotoxicity but also with resistance to platinum agents. A key feature of DNA repair is nucleotide excision at relatively well defined positions either side of the damaged site. The conformational flexibility of the interstrand cross-links is a general property of polynuclear platinum bifunctional DNA binding agents and this delocalization of the lesion, within an

(32) Bourdouxhe-Housiaux, C.; Colson, P.; Houssier, C.; Waring, M. J.; Bailly, C. *Biochemistry* **1996**, *35*, 4251−4264.
(33) Hansen, M.; Hurley, L. *J. Am. Chem. Soc.* **1995**, *117*, 2421−2429.
(34) McGregor, T. D.; Bousfield, W.; Qu, Y.; Farrell, N. *J. Inorg. Biochem.* **2002**, *91*, 212−219.
(35) Ohndorf, U.-M.; Rould, M. A.; He, Q.; Pabo, C. O.; Lippard, S. J. *Nature* **1999**, *399*, 708−712.

appropriate sequence, could represent an extremely efficient block to excision repair.

In summary, the kinetic and structural features deduced in this work reinforce the concept of a chemically unique set of interstrand cross-links with interesting implications for the biological processing and eventual "downstream" effects leading to cellular cytotoxic events. Continued investigation is warranted to delineate further the unique properties leading to the high cytotoxicity of compounds such as 1,0,1/t,t,t.

Acknowledgment. This work was supported by the Australian Research Council (to S.J.B.-P. and N.F.) and National Institutes of Health (RO1-CA78754), National Science Foundation (INT-9805552 and CHE-9615727) and the American Cancer Society (RPG89-002-11-CDD). We thank Dr Zijian Guo (Nanjing) for helpful discussions and Dr G. Pierens for assistance with NMR experiments.

Supporting Information Available: SCIENTIST models used to determine the rate constants given in Table 4, HPLC chromatograms of the unpurified final products from the reactions of **1** with duplex **I** and **II**, [^{1}H,^{15}N] and ^{1}H NMR spectra of the final products of both these reactions over the temperature range 288 K to 316 K, plots of the relative volumes of peaks assignable to the two conformers of the bifunctional adduct during reaction of ^{15}N-**1** with duplex **I** and molecular model illustrating the preassociation of **1** with duplex **II**. This material is available free of charge via the Internet at http://pubs.acs.org.

JA036105U